ELSEVIER

Mechanics of Materials 33 (2001) 603–616

MECHANICS OF MATERIALS

www.elsevier.com/locate/mechmat

A unified constitutive model for strain-rate and temperature dependent behavior of molybdenum

Jingyi Cheng [1], Sia Nemat-Nasser *, Weiguo Guo [2]

Department of Mechanical and Aerospace Engineering, Center of Excellence for Advanced Materials, University of California, San Diego, 4207 Engineering Bldg, Unit 1, 9500 Gilman Drive, La Jolla, CA 92093-0416, USA

Received 17 March 1999; received in revised form 30 July 2001

Abstract

In this paper, a constitutive model proposed by Cheng and Nemat-Nasser [Acta Mater. 48 (2000) 3131] is extended to describe both the dynamic and quasi-static stress–strain response of a commercially pure molybdenum over the temperature range 300–1100 K. Experimental results of Nemat-Nasser et al. [Acta Mater. 47 (1999) 3705; Scripta Mater. 40 (1999) 859] suggest that molybdenum behaves plastically differently at high and low strain rates. Within the framework of the classical theory of thermally activated dislocation motion, different models and model parameters must be used for high and low strain-rate deformations, indicating that different rate-controlling deformation mechanisms may be involved. In the present paper, a unified constitutive description of the mechanical behavior of molybdenum is developed. The activation energy and the maximum strength of the local barriers to the dislocation motion, change gradually with the changing strain-rate and temperature, due to the increased solute mobility with increasing temperature. Therefore, no change in the deformation mechanism is actually included. Only the configuration of the local obstacles is assumed to change because of the change in the solute mobility. The model predictions are in good agreement with the experimental results.

1. Introduction

Most metals' plastic response is strain-rate- and temperature-dependent. At a given strain-rate, the temperature dependence of the flow stress of crystalline solids has several distinctive characteristics. At low temperatures, the flow stress decreases rapidly with increasing temperature, until a plateau is reached at a temperature, say, T_L. Above T_L, there is a plateau within which the flow stress is almost independent of the temperature, the dependence being no greater than the temperature dependence of the shear modulus. To a certain extent, raising the strain-rate is equivalent to lowering the temperature for the plastic flow of metals. For almost all metals containing solute atoms (both interstitial and substitutional), the phenomenon of dynamic strain-aging is commonly observed at high temperatures and low strain rates. Within the regime of strain rates and

* Corresponding author. Tel.: +1-858-534-5930; fax: +1-858-534-2727.

E-mail address: sia@shiba.ucsd.edu (S. Nemat-Nasser).

[1] We report with sadness the sudden death of our coauthor, Professor Jingyi Cheng at the young age of 37, on February 14, 2000, in Hefei, China.

[2] Present address: Department of Aircraft Engineering, Northwestern Polytechnical University, Xian, Shaanx 710072, People's Republic of China.

0167-6636/01/$ - see front matter
PII: S0167-6636(01)00076-X

temperatures that dynamic strain-aging occurs, the flow stress is only minimally dependent on temperature. In certain cases, the flow stress may even increase with increasing temperature or decreasing strain-rate. One or several humps may be observed in the flow stress–temperature curve due to the different mobilities of different solute atoms. With a further increase in temperature, the flow stress again decreases rapidly with increasing temperature, because of the saturation nature of the dislocation core atmosphere.

The strain-rate- and temperature-dependent plasticity of crystalline solids stems from the thermal activation nature of the kinetics of dislocation slip and dynamic recovery. The kinetics of dislocation slip represents the instantaneous rate and temperature dependence of the material, and the kinetics of dynamic recovery represents the strain-rate- and temperature-history dependence of the material. Dynamic strain-aging phenomena are quite generally associated with the diffusion of solute atoms, arresting dislocations (Nemat-Nasser et al., 1999a,b; McCormick, 1971). To explain the experimentally observed dynamic strain-aging (van den Beukel, 1980) in a commercially pure titanium at high strain rates, Cheng and Nemat-Nasser (2000) suggested that the controlling mechanism may involve: (1) an increase in the solute atom density within the dislocation core region, which results from the capturing of new solute atoms by dislocations as they bow-out from their equilibrium position while waiting at the forest dislocation barriers; and (2) the diffusion of the solute atoms already existing in the core, with the dislocations under the strong interaction force between the dislocations and the solute atoms.

For applications involving various thermomechanical loading conditions, in addition to the dislocation density, a unified constitutive model must include the variation of the solute concentration as a state variable, in order to account for dynamic strain-aging. Usually, it is assumed that, the increase of the solute density in the dislocation core gives rise to an additive contribution, τ_d, to the flow stress (Estrin and McCormick, 1991; Kubin and Estrin, 1990), τ,

$$\tau = \tau_a + \tau^* + \tau_d, \tag{1}$$

where τ_a is the athermal stress (long-range athermal resistance to dislocation motion), and τ^* is the thermal part of the resistance to dislocation motion. *The model developed by* Cheng and Nemat-Nasser (2000) *uses a different approach. The effect of the accumulation of the core atmosphere on the flow stress is introduced indirectly through its influence on the thermal activation energy and the maximum local resistance to the dislocation motion, using Kocks' model of a "trough" for the thermally activated breakaway of dislocations from the core atmosphere* (Kocks, 1985).

Usually, the models which include dynamic strain-aging, are applied within narrow strain-rate and temperature ranges where the effects of dynamic strain-aging are significant. In this paper, the constitutive model of Cheng and Nemat-Nasser (2000) is extended to describe both the dynamic and quasi-static stress–strain response of commercially pure molybdenum over a temperature range 300–1100 K. Experimental results of Nemat-Nasser et al. (1999a,b) suggest that the plastic response of molybdenum is quite different at high and low strain rates. For this material, there are several dynamic strain-aging phenomena which occur at low strain rates within various temperature ranges due to different mobility of different solute atoms. In the present paper, a unified model for the mechanical behavior of molybdenum is presented. Here, the activation energy and the maximum strength of the local barriers to dislocation motion are assumed to change gradually with changing strain-rate and temperature, in order to account for the increase in the solute mobility at higher temperatures. Therefore, no change in the deformation mechanism is actually assumed. Only the configuration of the local obstacles is considered to change because of solute mobility, leading to a unified model. It is shown that the model predictions are in good agreement with the experimental results.

2. Constitutive model

According to Seeger (1958), the shear stress resisting plastic deformation is the sum of an athermal part, τ_a, which depends on temperature

such that τ_a/μ is temperature independent, and a thermally activated part, τ^*

$$\tau = \tau_a + \tau^*, \tag{2}$$

where μ is the shear modulus. The mechanical threshold stress, i.e., the flow stress at "zero temperature", is expressed as:

$$\hat{\tau} = \tau_a + \hat{\tau}^*, \tag{3}$$

where $\hat{\tau}^*$ is the maximum strength of the local obstacles to the motion of dislocations. The additive assumption in (2) and (3) implies the existence of two sets of independent obstacles that are activated during the motion of dislocations. The first set corresponds to the elastic field of all lattice defects which produce an "athermal" stress field. The athermal resistance cannot be overcome by thermal activation. Its temperature dependence corresponds to the weakly temperature dependence of the elastic field of defects. The second set consists of weak obstacles that can be overcome by thermal activation, with the assistance of the applied stress. At finite temperatures and strain rates, the strength of the local obstacles is changed to a measurable effective value, τ^*, given by

$$\tau^* = s(\dot{\gamma}, T)\hat{\tau}^*, \tag{4}$$

where $s(\dot{\gamma}, T)$ is a function with the maximum value of 1 as $T \to 0$, and the minimum value of 0 as $T \to T_s$, where T_s is the temperature above which local barriers no longer present any resistant to the dislocation motion; $\dot{\gamma}$ is the plastic strain-rate; and T is the absolute temperature.

Kocks et al. (1975) have given a comprehensive review of various factors that must be considered to properly describe the thermodynamics and kinetics of slip. They suggest that the stress factor $s(\dot{\gamma}, T)$ in Eq. (4), can be generally expressed as:

$$s(\dot{\gamma}, T) = \left[1 - \left(-\frac{kT}{F_0}\ln\frac{\dot{\gamma}}{\dot{\gamma}_0}\right)^{1/q}\right]^{1/p}, \tag{5}$$

where F_0 is the *total* free energy necessary to overcome the obstacle without the aid of an externally applied stress, k is Boltzmann's constant, $0 < p \leqslant 1$ and $1 \leqslant q \leqslant 2$ are parameters representing the profile of the obstacle, and $\dot{\gamma}_0 = \beta b \rho_m l v_0$ is generally considered a constant; here β is the orientation factor, b is the magnitude of the Burgers vector, ρ_m is the density of the mobile dislocations, l is the average distance the dislocations travel after a successful activation event, and v_0 is the attempt frequency of the dislocation segment. The physical reason for $\dot{\gamma}_0$ being viewed as a constant is that a decrease in the dislocation free path is partially compensated for by an increase in the mobile dislocation density. In addition, the mathematical structure of (5) is such that, a small variation of $\dot{\gamma}_0$ does not affect the function $s(\dot{\gamma}, T)$ in a substantial way.

To relate the physical parameters $\hat{\tau}^*$ and F_0 to the microstructural state of the material, a detailed model for the interaction between dislocations and local obstacles opposing the motion of dislocations, is needed. For BCC metals, the effect of solute atoms on the movement of dislocations is a complex phenomenon. At low temperatures, instead of solute hardening, solute softening is also observed for dilute solute concentrations in BCC metals. Nevertheless, solute hardening is generally observed at intermediate to high temperatures. In the present case, the considered temperature range is from room temperature to 1100 K (Nemat-Nasser et al., 1999a,b). Hence, solute hardening (rather than softening) can be safely assumed. The rate-controlling mechanism for BCC metals at low temperatures is the thermally activated dislocation motion over the Peierls–Nabarro potential. The presence of solute atoms in the dislocation core area changes the amplitude of the Peierls–Nabarro potential. Assuming that, the effective potential energy is F_B, within the framework of the *trough model* (Kocks, 1985), the physical parameters F_0 and $\hat{\tau}^*$ are assumed to relate to the properties of dislocations and obstacles as follows:

$$F_0 \propto \sqrt{F_D F_B}\, w \tag{6}$$

and

$$\hat{\tau}^* \propto \frac{F_0}{b l_b w}, \tag{7}$$

where F_D is the free energy per unit length of the dislocation free of the effects of solutes and Peierls–Nabarro potential, w is the effective width

of the trough, and l_b is the bulge length. Due to workhardening, the bulge length is limited by the link length of dislocations, say, l_d. Therefore, l_b is equal to [3] l_d. The effective potential energy, F_B, is assumed to be proportional to the effective interaction strength of each solute atom, F_{B0}, times the concentration of solutes along the dislocation line, C

$$F_B \propto F_{B0} C. \tag{8}$$

Here, the effective interaction strength of each solute atom, F_{B0}, contains the binding energy of solute atom with dislocation and the Peierls–Nabarro potential that is partitioned to each solute atom. Therefore, the solute-concentration dependence of the thermal activation energy and the mechanical threshold stress can be expressed as follows:

$$F_0 = F_0' \sqrt{\frac{C}{C_0}} \tag{9}$$

and

$$\hat{\tau}^* = \tau_0 \sqrt{\frac{C}{C_0}} \left(\frac{l_0}{l_d} \right), \tag{10}$$

respectively. Here F_0' is the activation energy at a solute concentration of C_0, and $\tau_0 = F_0'/bl_0w$ is a constant, with l_0 and l_d being the initial and current average dislocation link length. According to Kuhlmann-Wilsdorf (1999), the link length of dislocation is related to the dislocation density by $l_d \propto 1/\sqrt{\rho}$, i.e., $(l_d/l_0) = (\rho_0/\rho)^{1/2}$, where ρ_0 and ρ are the initial and current dislocation densities.

The essence of bulge nucleation is that the length of the dislocation "bulge" is not related to the spacing of individual solute atoms: the bulge is a breakaway from a trough. The solutes behave as if they were smeared out along the dislocation, and only their interaction energy per unit length matters. This energy is proportional to the interaction strength of each solute atom times the concentration along the dislocation line.

To complete the description of the plastic behavior of the material, the evolution of the structural parameters, such as the dislocation segment length l_d, the athermal resistance to the dislocation motion, τ_a, and the concentration of solutes along the dislocation line, C, must be quantified.

2.1. Variation of the average length of dislocation segments

The variation of the average length of dislocation segments relates to the workhardening of the material. Nemat-Nasser and Li (1998) have proposed a simple empirical model to estimate this average length. Assuming that the average dislocation spacing is a decreasing function of the accumulated plastic strain and an increasing function of the temperature, the variation of the average length of the dislocation segments is expressed as:

$$l_d = \frac{l_0}{f(\gamma, T)} \tag{11}$$

with the following constraining conditions for the dimensionless function f:

$$f(\gamma, T) > 0, \quad f(0, T_0) = 1,$$
$$\frac{\partial f(\gamma, T)}{\partial \gamma} \geqslant 0, \quad \frac{\partial f(\gamma, T)}{\partial T} \leqslant 0, \tag{12}$$

where γ is the plastic strain (used here as a time parameter [4]), and T_0 is the initial temperature. As

[3] A simple estimate of the bulge length can be made as follows. The activation energy is related to the temperature and strain-rate through the Arrhenius equation,

$$\Delta G = kT \ln(\dot{\gamma}_0/\dot{\gamma}). \tag{a}$$

The stress dependence of ΔG can be expressed as:

$$\Delta G = F_0 - \tau bwl_b \approx F_0 - \tau b^3 (l_b/b). \tag{b}$$

With the use of the typical values involved in the above equations, i.e., $\ln(\dot{\gamma}_0/\dot{\gamma}) \approx 20$, $F_0 \approx 1$ eV, at room temperature, $kT \approx 0.02$ eV, and $\tau b^3 \leqslant \mu b^3/1000 \approx 1/250$ eV, we have

$$l_b = \frac{F_0 - kT \ln(\dot{\gamma}_0/\dot{\gamma})}{\tau b^3} b \geqslant 150b. \tag{c}$$

For metals with the typical dislocation density $\rho = 10^{15}$ m^{-2}, the dislocation link length should be $l_d \approx 100b$. The bulge length cannot be greater than the dislocation link length, because the dislocation nodes are strong obstacles to dislocation motion. Therefore, we have

$$l_b = l_d. \tag{d}$$

[4] Note that, while $l_d/l_0 = (\rho_0/\rho)^{1/2}$ can be a state parameter, the plastic strain, γ, is generally used as a "time parameter" and not as a state parameter.

an example, the following empirical relations are used in Nemat-Nasser and Li (1998) for application to OFHC copper

$$l_d = \frac{l_0}{1 + a(T)\gamma^{n_0}} \tag{13}$$

and

$$a(T) = a_0\left[1 - \left(\frac{T}{T_m}\right)^2\right]. \tag{14}$$

Here, a_0 and n_0 are viewed as constitutive parameters, with n_0 between 0 and 1, and T_m is the melting temperature.

In this paper, another empirical relation for $a(T)$

$$a(T) = a_0\left[1 - \frac{T}{T_0}\right] \tag{15}$$

is used. Here, T_0 is a constant temperature, chosen such that the resulting function f satisfies conditions (12).

2.2. Athermal resistance

The athermal resistance to the dislocation motion represents the long-range effect of all other dislocations, grain boundaries, and defects. It is expressed by the following empirical relation:

$$\tau_a = g(\gamma, d_G, \ldots)\tau_a^0, \tag{16}$$

where d_G is the average grain size, τ_a^0 is a constant with the dimension of stress, and g is a dimensionless function of the indicated arguments. In this paper, it is assumed that

$$\tau_a = \tau_a^0\gamma^{n_1}, \tag{17}$$

where n_1 is a constant. Note again that the plastic strain γ is used here as a time parameter.

2.3. Solute concentration on dislocation lines

A key to a quantitative description of dynamic strain-aging is to model the variation of the solute concentration on the dislocation lines. Due to the extreme complexity of the process of interaction between solute atoms and dislocations, the exact theoretical model for the variation of the dislocation core atmosphere is very difficult to formulate. For dilute solute concentrations, Cottrell and Bilby (1949) developed a theory of strain-aging in iron, based on the segregation of carbon atoms which temporarily arrest the dislocations. According to Cottrell–Bilby strain-aging kinetics, the solute concentration on a dislocation line, C, may be expressed as:

$$C = C_0\left(\frac{t_w}{t_D}\right)^{2/3}, \tag{18}$$

where C_0 is the alloy solute composition, t_w is the average waiting time of dislocations at the obstacles, $t_D = 1/(KD)$ is the characteristic diffusion time, with D being the solute diffusion coefficient, and K is a constant which includes the solute–dislocation binding energy. Eq. (18) is valid only for the initial stages of aging. Louat (1981) generalized the Cottrell–Bilby kinetics to include saturation at long aging times. The local concentration C may now vary between the nominal value, C_0, and the saturation concentration, C_s, with the characteristic diffusion time, t_D

$$\frac{C}{C_0} = 1 + \left(\frac{C_s}{C_0} - 1\right)\left\{1 - \exp\left[-\left(h_0\frac{t_w}{t_D}\right)^{\alpha}\right]\right\}, \tag{19}$$

where h_0 is a proportionality parameter. The exponent α equals 1/3 or 2/3, depending on the diffusion mechanisms of the solute atoms, the former corresponding to pipe diffusion along the dislocation line or dislocation bowing out and capturing solutes, and the latter corresponding to the volume diffusion in the crystal lattice (Cheng and Nemat-Nasser, 2000; Mesarovic, 1995). Because different solute atoms have different diffusion mobility, we generalize Eq. (19) as follows:

$$\frac{C}{C_0} = 1 + \sum_{i=1}^{n}\left(\frac{C_s i}{C_{0i}} - 1\right)\left\{1 - \exp\left[-\left(h_{0i}\frac{t_w}{t_{Di}}\right)^{\alpha_i}\right]\right\} \tag{20}$$

here and hereinafter the subscript i is used to indicate the corresponding quantity for the ith solute atom, and there are n types of solutes. Considering the uncertainties involved in the variation of both

mobile and total dislocation densities, we view (and use) Eq. (20) as a "working" assumption.

When the plastic strain-rate is constant, the average waiting time has a steady-state value. According to Orowan's equation, neglecting the running time of the dislocation between obstacles, the average waiting time is related to the plastic strain-rate, by

$$t_{\mathrm{w}} = \frac{\dot{\gamma}_0}{v_0 \dot{\gamma}}, \quad \dot{\gamma}_0 = \beta b \rho_{\mathrm{m}} l v_0. \tag{21}$$

The characteristic diffusion time, $t_{\mathrm{D}i}$, can be generally expressed as:

$$t_{\mathrm{D}i} = \frac{1}{v'_{0i}} \exp\left(- \frac{Q_i - Q_{\mathrm{c}i}}{kT} \right), \tag{22}$$

where Q_i is the activation energy for the diffusion of the ith solute atom, v'_{0i} is the corresponding attempt frequency, and $Q_{\mathrm{c}i}$ is the total interaction energy between a dislocation and the ith solute atom during its diffusion to or along the dislocation. According to the mechanism of the dislocation and solute interaction, $Q_{\mathrm{c}i}$ can be written as

$$Q_{\mathrm{c}i} = \tau b l^* a_i^* \quad \text{when } \tau b l^* a_i^* < Q_{\mathrm{B}i} \tag{23}$$

or as

$$Q_{\mathrm{c}i} = Q_{\mathrm{B}i} \quad \text{when } \tau b l^* a_i^* > Q_{\mathrm{B}i}. \tag{24}$$

Here, a_i^* is the width of the potential for a solute atom diffusion, $l^* = 1/C$ is the average spacing between the solute atoms along the dislocation core, $\tau b l^* = \tau b / C$ is the force exerted on each of the core solutes by the dislocation, and $Q_{\mathrm{B}i}$ is the binding energy between the dislocation and the solute atoms. For the process of solute diffusion to the dislocation core under the elastic field of dislocation, the diffusion time is

$$t_{\mathrm{D}i} = \frac{1}{K_i D_i}. \tag{25}$$

When solute atoms diffuse to a dislocation core under the action of the elastic field of the dislocation, then the saturation concentration of the core atmosphere depends only on the core sites available and the solute atom concentration. Therefore, it should be a constant. On the other hand, when diffusion of solute atoms occurs during the movement of the dislocation and when new solute atoms are captured by the moving dislocation, then the saturation concentration depends on the area that the dislocation sweeps under the equilibrium bowing-out of its segments. A simple description of this behavior has been proposed in (Cheng and Nemat-Nasser, 2000). For the ith solute, this becomes,

$$\frac{C_{si}}{C_{0i}} - 1 = C_i \left(\frac{\tau - \tau_{\mathrm{a}}}{\tau_i C / C_0} \frac{\gamma}{\gamma_i} \exp\left(1 - \frac{\gamma}{\gamma_i} \right) \right)^{n_{2i}}, \tag{26}$$

where C_i, τ_i, γ_i, and n_{2i} are constants.

Based on the above analysis, the final constitutive relation is now expressed as follows:

$$\dot{\gamma} = \dot{\gamma}_0 \exp\left\{ - \frac{F'_0 \sqrt{C/C_0}}{kT} \left[1 - \left(\frac{\tau - \tau_{\mathrm{a}}}{\tau'_0 \sqrt{C/C_0}\, l_0 / l_{\mathrm{d}}} \right)^p \right]^q \right\} \tag{27}$$

with

$$\frac{l_0}{l_{\mathrm{d}}} = f(\gamma, T) = 1 + a_0 \left(1 - \frac{T}{T_0} \right) \gamma^{n_0}, \tag{28}$$

$$\tau_{\mathrm{a}} = \tau_{\mathrm{a}}^0 \gamma^{n_1}, \tag{29}$$

$$\frac{C}{C_0} - 1 = \sum_{i=1}^{n} \left(\frac{C_{si}}{C_{0i}} - 1 \right) \left\{ 1 - \exp\left[- \left(\frac{\Omega_i}{\dot{\gamma}} \exp\left(- \frac{Q_i - Q_{\mathrm{c}i}}{kT} \right) \right)^{\alpha_i} \right] \right\}, \tag{30}$$

and

$$\frac{C_{si}}{C_{0i}} - 1 = C_i \left(\frac{\tau - \tau_{\mathrm{a}}}{\tau_i C / C_0} \frac{\gamma}{\gamma_i} \exp\left(1 - \frac{\gamma}{\gamma_i} \right) \right)^{n_{2i}}, \tag{31}$$

where $\Omega_i = h_{0i} \beta b \rho_{\mathrm{m}} l v'_{0i} = h_{0i} \dot{\gamma}_0 v'_{0i} / v_0$ is a material parameter.

With $n = 1$, the above model reduces to that of Cheng and Nemat-Nasser (2000), in which only one mobile solute is considered. When the solute concentration along the dislocation line does not vary with time (in the case when the solute atoms are immobile, or are saturated at high temperatures), the above equation reduces to the model of Nemat-Nasser and Li (1998), with only a minor difference, i.e., in the present paper, the reference strain-rate $\dot{\gamma}_0$ is considered to be a constant,

whereas in Nemat-Nasser and Li (1998) assume it to be proportional to the current value of the average dislocation spacing, l.

3. Determination of model constants and comparison with experimental results

3.1. Determination of model constants

To evaluate the model constants, we first note that the experimental stress–temperature curves suggest that the corresponding location of the three humps along the temperature axis, is almost independent of the strain. Then, the exponents n_{2i} should be close to zero. This is in contrast to the dynamic strain-aging observed at high strain rates in titanium (Cheng and Nemat-Nasser, 2000; Nemat-Nasser et al., 1999a,b), which is strongly dependent on the strain. Therefore, in the present case, we may simplify the model to

$$\tau = \tau_0' \sqrt{\frac{C}{C_0}} \left\{ 1 - \left[-\frac{kT}{F_0' \sqrt{C/C_0}} \left(\ln \frac{\dot{\gamma}}{\dot{\gamma}_0} \right) \right]^{1/q} \right\}^{1/p} \times \left[1 + a_0 \left(1 - \frac{T}{T_0} \right) \gamma^{n_0} \right] + \tau_a^0 \gamma^{n_1} \tag{32}$$

and

$$\frac{C}{C_0} = 1 + \sum_{i=1}^{n} C_i \left\{ 1 - \exp \left[- \left(\frac{\Omega_i}{\dot{\gamma}} \exp \left(- \frac{Q_i - Q_{ci}}{kT} \right) \right)^{\alpha_i} \right] \right\}. \tag{33}$$

For dynamic loading, the temperature rise due to adiabatic heating must be included. Here, we assume that 95% of the total plastic work is used to increase the temperature of the sample, the remaining part being lost by conduction or other means. As shown by Kapoor and Nemat-Nasser (1998), and verified by Nemat-Nasser et al. (1999a,b) for the present molybdenum, essentially all the inelastic energy associated with the plastic work is converted into heat at suitably large strains, with an insignificant amount being stored as the elastic energy of defects.

Usually, it is rather difficult to determine the material parameters in inelastic constitutive equations, especially when the physical meaning of the parameters is not fully understood. The more empirical relations are introduced, the more complex the identification of the constitutive parameters becomes.

On the other hand, physically based models which include parameters that relate to well understand deformation mechanisms on the microscopic or atomic scale, are easy to relate to the experimental results. In the constitutive relation proposed by Cheng and Nemat-Nasser (2000), when the solute mobility is low and there is little variation in the dislocation core atmosphere, then the model reduces to that developed by Nemat-Nasser and Li (1998). This case corresponds to the low-temperature regimes. For cases in which solute mobility does not affect the material response, Nemat-Nasser and Isaacs (1997), suggest an effective way to determine the model parameters. When the solute mobility must be included, then the determination of the material parameters is somewhat more complex, although the same method may be used as a starting point.

Kocks et al. (1975) have pointed out that essentially all barrier profiles of interest can be modeled by proper choice of the exponents p and q in (32). Experimental results suggest that $p = 2/3$ and $q = 2$ are suitable values for local barriers to dislocation motion. These values for p and q are used in the present paper. The experimental results show clearly that there are three humps in the flow stress vs temperature curves, indicating that at least three dynamic strain-aging processes must occur at three different temperatures. As it will be explained later, according to the analysis of Kocks (1985), the departure of the low-temperature behavior under quasi-static loading from the classical theory of thermally activated dislocation motion, also stems from the solute mobility. Therefore, the number n in Eq. (20) is 4. The remaining parameters are determined to best fit the experimental results.

At high strain rates and low temperatures, the solutes have limited mobility. In this regime, the classical theory of thermally activated dislocation

motion, directly applies. Therefore, the flow stress vs temperature curves for these regimes can be used to determine the activation energy, F_0', and the reference strain-rate, $\dot{\gamma}_0$. In the ideal cases when no solute mobility is involved at high temperatures, one expects that the high-temperature results can be used to fix the constitutive parameters, n_1 and τ_0^a, which define the athermal part of the flow stress in Eq. (32), since the flow stress then should be independent of the strain-rate and temperature (Nemat-Nasser and Isaacs, 1997). However, the experimental results for molybdenum show that, even at very high temperatures, the flow stress still weakly depends on the strain-rate and temperature; see Fig. 1. Therefore, the athermal part of the flow stress cannot be easily determined from high-temperature alone. To overcome this difficulty, we use the low-temperature data to determine the athermal part of the flow stress. At low temperatures, effects due to solute mobility are absent. The model reduces to that of Nemat-Nasser and Li (1998). By best fitting the low-temperature data at both high strain rates and low strain rates, the parameters of both the thermal and athermal parts of the flow stress are evaluated. Extrapolating the results of this low-temperature fit to high-temperature regimes, it is observed that the model predictions of the flow stress would be lower than those experimentally observed. The difference between the model prediction and the experiments is then assumed to be due to the contribution of mobile solute atoms. In this manner, the parameters for the variation of the dislocation core atmosphere are determined.

Once the model parameters that are associated with the standard theory of thermally activated deformation, are determined from the low-temperature data, the equations are used to predict the high-temperature response, in which the effects of the solute mobility are present. The difference between the actual and predicted flow stresses is then attributed to the solute mobility. In the model of Cheng and Nemat-Nasser (2000), the effects due to the solute mobility are represented through the effects of the variation of the concentration of the dislocation core atmosphere on the thermal activation energy and the mechanical threshold stress.

It should be noted that, under quasi-static loading, the positions of the humps along the temperature coordinate, remain the same, regardless of the strain-rate; see Figs. 1–3. If the parameter Ω_i is constant, then the temperatures at which a hump occurs should shift to higher values as the strain-rate is increased. Therefore, to accu-

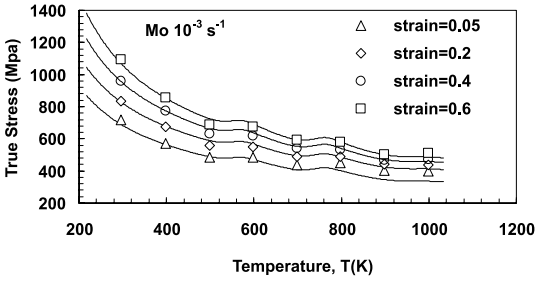

Fig. 2. Flow stress vs temperature curves for molybdenum at indicated plastic strain (symbols: experimental, solid lines: theoretical).

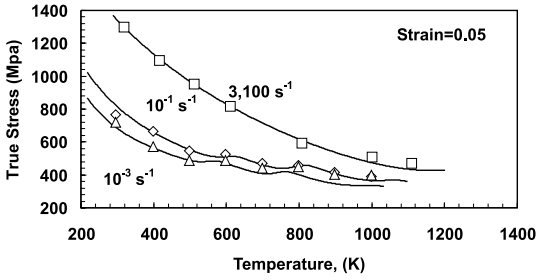

Fig. 1. Flow stress vs temperature curves for molybdenum at indicated plastic strains (symbols: experimental, solid lines: theoretical).

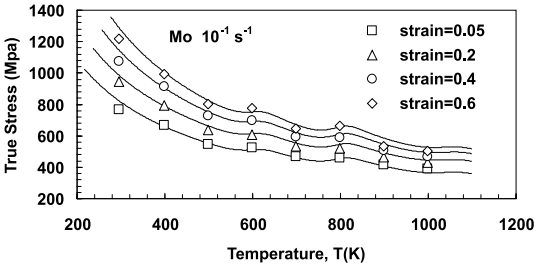

Fig. 3. Flow stress vs temperature curves for molybdenum at indicated plastic strains (dotted lines: experimental, solid lines: theoretical).

rately predict the position of the humps along the temperature coordinate, the variation of Ω_i with loading conditions (such as strain-rate, stress, temperature, and strain) should be included. The variation of Ω_i has a significant influence on the kinetics of solute–dislocation interaction. Experimental results indicate that the expected relation for Ω_i is complicated. From Figs. 1–3, one finds that, while the humps remain stationary under quasi-static loading, they do disappear under dynamic loading over the same temperature range. This means that, under dynamic loading conditions, the humps indeed shift to higher temperatures, outside the temperature range used in the experiments. To include the above facts in the model, the following expression is proposed here to relate the parameter Ω_i to the strain-rate

$$\Omega_i = \Omega_i' \left(\frac{\dot{\gamma}}{\dot{\gamma}_{00}} \right)^{m \exp(-\dot{\gamma}/\dot{\gamma}_{00}) - m_0}, \tag{34}$$

where Ω_i', m, and m_0 are constants, and $\dot{\gamma}_{00}$ is a reference strain-rate. Through best fitting, the remaining parameters can now be determined. The model parameters are summarized in Table 1.

3.2. Comparison with experimental results and discussion

The experimental procedure and results have been reported elsewhere by Nemat-Nasser et al. (1999a,b). Here, our focus is on the mechanical behavior of molybdenum over a broad range of loading conditions, where dynamic strain-aging occurs. Fig. 1 shown by the various geometric symbols the experimentally obtained variation of the flow stress with the temperature, for strain rates of 3100, 10^{-1}, and 10^{-3} s^{-1}, at a 0.05 plastic strain. The solid curves are the corresponding theoretical predictions. As is seen, good correlation between the experimental and model results is obtained. Figs. 2 and 3 show the stress–temperature relations for strain rates of 10^{-1} and 10^{-3} s^{-1}, at indicated plastic strains. Stress–strain curves at different strain rates and temperatures are shown in Figs. 4–7. All these results show that the model adequately captures the main features of the observed response of this material. This is especially evident in Figs. 1–3, where the humps in the stress–temperature curves are adequately modeled by the constitutive relation. As is seen, with the same model parameters, the model results fit the experimental data over a broad range of strain rates and temperatures.

Table 1
Summary of material constants

Constants	Values	Constants	Values
τ_0'	2500 MPa	F_0'	96.41 kJ/mol
p	2/3	q	2
$\dot{\gamma}_0$	2×10^7 s^{-1}	a_0	1.5
n_0	1	τ_a^0	520 MPa
n_1	0.15	T_0	1700 K
$Q_1 - Q_{c1}$	30 kJ/mol	C_1	4.2
Ω_1'	0.5 s^{-1}	α_1	1/3
$Q_2 - Q_{c2}$	110 kJ/mol	C_2	0.26
Ω_2'	1×10^9 s^{-1}	α_2	1
$Q_3 - Q_{c3}$	190 kJ/mol	C_3	0.5
Ω_3'	1×10^{12} s^{-1}	α_3	1
$Q_4 - Q_{c4}$	250 kJ/mol	C_4	0.6
Ω_4'	1×10^{12} s^{-1}	α_4	1
m	0.8	m_0	0.25

3.2.1. The influence of solute mobility on flow stress

Like most metals, the temperature dependence of the flow stress of molybdenum has several features. There is a significant drop in the flow stress as the temperature is increased in the low-temperature regimes, followed by a flow stress "plateau" at higher temperatures. The transition between the two regimes occurs at about or a little above the room temperature, under quasi-static deformation conditions; see Fig. 1. Under dynamic loadings, this transition moves to higher temperatures. At low strain rates and high temperatures, humps are seen in the flow stress vs temperature diagrams; see Figs. 1–3.

The plateau and "humps" in the flow stress vs temperature relation are assumed to be due to the solute mobility (Kocks, 1985; Gleiter, 1968; Cuddy and Leslie, 1972; Neuhäuser and Flor, 1978; Schwarz, 1979; van den Beukel, 1983). Above certain temperatures, solutes become mobile, tending to segregate to dislocations. This increases the concentration of the solute atmosphere in the dislocation core. According to Eqs. (8) and (9), this increases the activation energy, F_0, and the maxi-

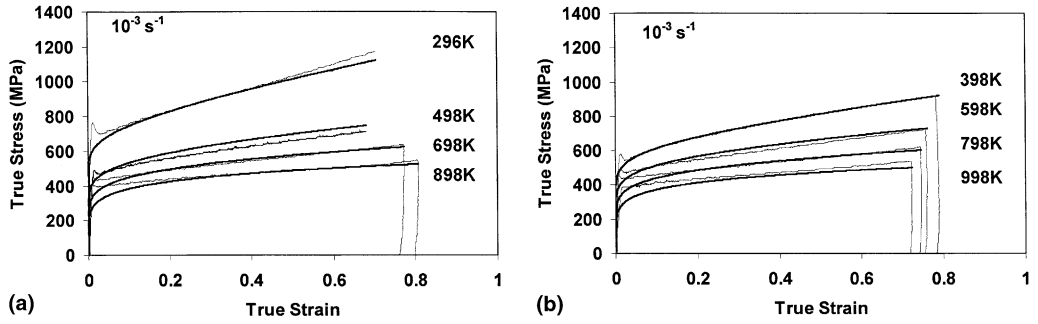

Fig. 4. Experimental (thin solid) and model (thick solid) stress–strain curves.

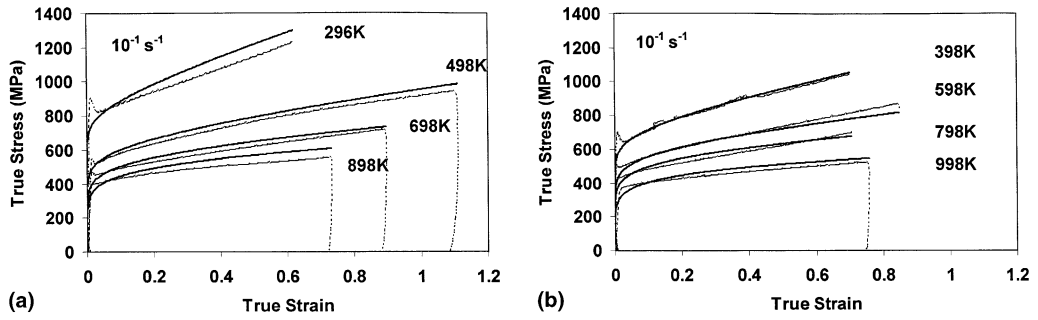

Fig. 5. Experimental (dotted) and model (thick solid) stress–strain curves.

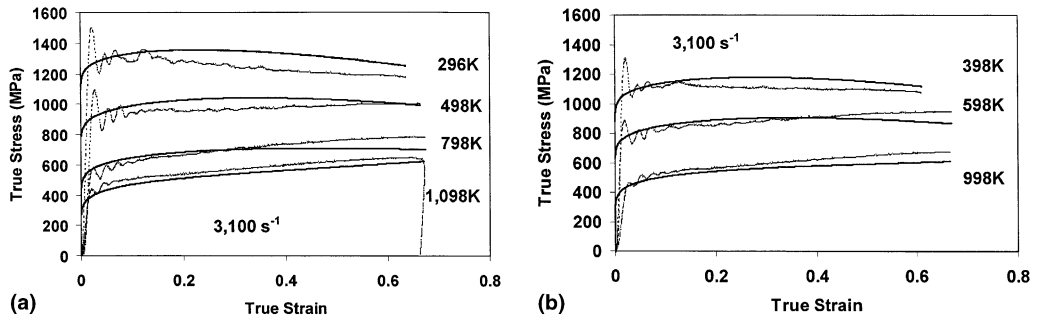

Fig. 6. Experimental (dotted) and model (thick solid) stress–strain curves.

mum strength of the local obstacles to dislocation motion. Therefore, the stress required to further deform the material is greater than at the same temperature but for lower solute atmosphere concentration in the dislocation core. In the temperature range where there is sufficient solute mobility, the increase of the activation energy and the strength of the local barrier, may compensate for the thermal softening effect due to a temperature rise. Therefore, a plateau or even a hump in the flow stress vs temperature relation occurs. If the difference in the mobilities of different solute

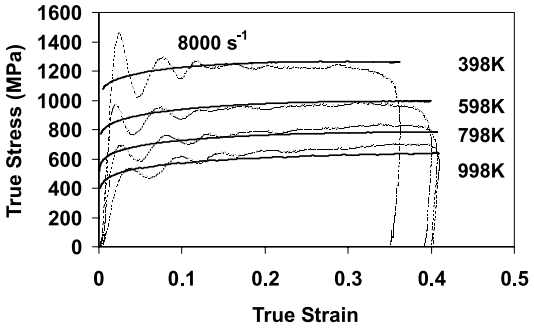

Fig. 7. Experimental (broken) and model (thick solid) stress–strain curves.

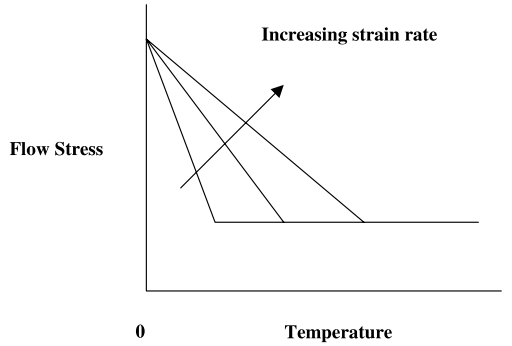

Fig. 8. Sketch of the dependence of flow stress on temperature at different strain rates under the framework of classical theory of thermal activation.

atoms is large, then several humps in the flow stress vs temperature may be observed. In the present case, three humps are experimentally observed and are theoretically modeled. Due to the lack of data about the interaction energy between dislocations and solute atoms, no attempt is made here to identify which solute is responsible for which of the observed hump. After the dislocation core atmosphere is saturated, the behavior of the material returns to the normal thermal softening, in line with the prediction of the classical theory of thermally activated dislocation motion.

The mobility of the solute atoms affects not only the high-temperature behavior of metals at low strain rates, but also the high-temperature behavior at high strain rates. At high strain rates, the influence zone of the solute mobility moves to higher temperatures, as compared to that at low strain rates. According to our model, the athermal part of the flow stress is lower than the measured flow stress at high temperatures, both for high strain-rate and low strain-rate deformations. The difference is due to the contribution of the solute mobility. Only after this fact is recognized, it is possible to reach a unified description of the mechanical behavior of metals over a broad range of strain rates and temperatures. Otherwise, different models have to be used for high and low strain rates.

Solute mobility has a significant influence on the flow stress under quasi-static loading in the temperature range from room to that of the plateau transition. If there is no effect of the solute mobility, then according to the classical theory of thermally activated dislocation motion, the lower is the strain-rate, the greater becomes the gradient of the flow stress vs temperature curves, as depicted in Fig. 8. But, in the case of the molybdenum studied here, and many other metals containing solute atoms, the inverse phenomenon actually occurs. The reason for this is the presence of the solute mobility. Because of the increase in solute mobility with a decrease in the strain-rate, the concentration of the dislocation core atmosphere increases. This results in an increase in the activation energy for dislocation slip, leading to a smaller gradient in the flow stress vs temperature curve. This fact is predicted by the proposed model.

3.2.2. Mechanism of dynamic strain-aging

A key feature of thermally activated dislocation motion is that the dislocations spend most of their time to interact with local obstacles, such as forests of dislocations, vacancies, and solute atoms. This period of time is called the waiting time in the literature. After the dislocation overcomes a set of obstacles, it runs very fast until it is stopped at the next group of obstacles. The average velocity of the dislocation is determined by the spacing between the obstacles and the waiting time spent during the thermal activation process. The dislocation moves in a

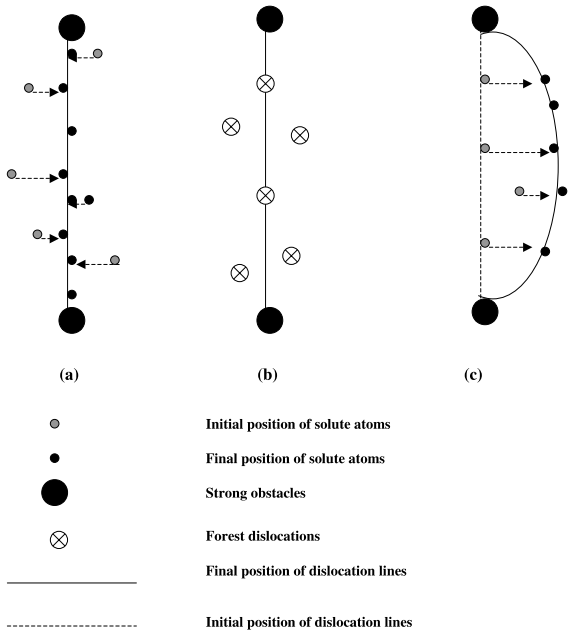

Fig. 9. Mechanisms of accumulation of core atmosphere: (a) solute atoms diffusing to the dislocation; (b) drainage of solute atoms through forest dislocations; (c) solute atoms diffusion along with the bowing-out movement of dislocation and new solutes captured by dislocation.

jerky way. The segregation of solute atoms to the dislocation core occurs during the time when the dislocations are waiting at the local obstacles.

There are several ways for the solute atoms to segregate into the dislocation core. Fig. 9 schematically depicts this situation. First, the solute atoms can diffuse to the dislocations via volume diffusion through the crystal lattice under the elastic interaction between dislocations and solute atoms. In this case, the dislocations are waiting passively for the solutes to diffuse to them and to form an atmosphere around them. Secondly, the solute atoms may reach the dislocation core via pipe diffusion along the forest dislocation lines. This is a fast diffusion process for substitutional atoms, having much lower activation energy than that of volume diffusion. A third mechanism proposed by Cheng and Nemat-Nasser (2000) is that the dislocations are not waiting passively for the solutes to diffuse to them, but rather they capture the solutes during their bowing-out process, under the applied stress, while being pinned down at dislocation forests. The increase in the concentration of the dislocation core atmosphere is a result of the diffusion of the existing core atmosphere along with the dislocation, and the new solutes that are encountered and captured by the dislocation. Because a strong interaction force between dislocations and solutes exists in the dislocation core area, the diffusion of the core atmosphere becomes significant at much lower temperatures than is possible for the solute atoms situated outside the core area, provided that the resolved shear stress on the dislocations is high enough.

4. Conclusions

1. The unified constitutive model of Cheng and Nemat-Nasser (2000) is extended to describe the dynamic and quasi-static stress–strain properties of a commercially pure molybdenum, over a temperature range 300–1100 K. The model combines the concepts of athermal long-range and thermally activated short-range barriers, with the Kocks model of a trough (Kocks, 1985) for the thermally activated breakaway of dislocations from the core atmosphere. The variation of the core atmosphere concentration is included in the model, based on the strong interaction force between dislocations and point defects in the core area.
2. Comparison of the model predictions and the experimental results shows that the model adequately captures the main features of the observed response of this commercially pure molybdenum. The humps in the stress–temperature curves, due to different solute mobilities of different solute atoms, are adequately described by the model.
3. It is noteworthy that a single model with the same model parameters fits the experimental results over a broad range of strain rates and temperatures. The temperature dependence of the flow stress appears to be different at high

and low strain rates, suggesting that different rate-controlling mechanisms may be involved. However, it is proposed that, due to the increased solute mobility at higher temperatures, the activation energy and the maximum local barrier strength for dislocation motion, change gradually with changing strain rate and temperature. Therefore, a change in the deformation mechanism is not actually involved, and the observed behavior of this molybdenum can be represented by a unified model. But one can still distinguish different temperature ranges in which different micro-processes have the dominant role. At low temperatures, when there is no solute mobility to appear, the behavior of metals is described by the classical theory of thermal activation. At high temperatures, theoretically speaking, only the athermal part of the flow stress provides the resistance to the motion of dislocations. In the experimental data cited here, this behavior has not been observed. It may be beyond the temperature range used in the experiments. The departure of the behavior from the classical theory of thermal activation, the plateau, and the humps are dynamic strain-aging phenomena due to the solute mobility. The different part of the model represents the different physics involved, so that the material constants can be relatively easily determined.

4. The variation of Ω_i has a significant influence on the kinetics of solute–dislocation interaction. Therefore, to accurately predict the shape of the flow stress vs temperature curves, the variation of Ω_i with loading conditions (such as strain-rate, stress, temperature, and strain) should be considered in modeling the variation of the dislocation core-atmosphere concentration.

Acknowledgements

This research was supported by the Center of Excellence for Advanced Materials, Department of Mechanics and Aerospace Engineering, University of California, San Diego.

References

Cheng, J.Y., Nemat-Nasser, S., 2000. A model for experimentally-observed high-strain-rate dynamic strain aging in titanium. Acta Mater. 48, 3131–3144.

Cottrell, A.H., Bilby, B.A., 1949. Dislocation theory of yielding and strain ageing of iron. Proc. Phys. Soc. LXII (I-A), 49–62.

Cuddy, L.J., Leslie, W.C., 1972. Some aspects of serrated yielding in substitutional solid solutions of iron. Acta Metall. 20, 1157–1167.

Estrin, Y., McCormick, P.G., 1991. Modelling the transient flow behaviour of dynamic strain ageing materials. Acta Metall. Mater. 39, 2977–2983.

Gleiter, H., 1968. Ausscheidungshärtung durch diffusion im spannungsfeld einer versetzung (Precipitation hardening by diffusion in the stress field of a dislocation). Acta Metall. 16, 857–861.

Kapoor, R., Nemat-Nasser, S., 1998. Determination of temperature rise during high strain rate deformation. Mech. Mater. 27, 1–12.

Kocks, U.F., 1985. Kinetics of solution hardening. Metall. Trans. A 16, 2109–2129.

Kocks, U.F., Argon, A.S., Ashby, M.F., 1975. Thermodynamics and kinetics of slip. Prog. Mater. Sci. 19, 68.

Kubin, L.P., Estrin, Y., 1990. Evolution of dislocation densities and the critical conditions for the Portevin-Le Chatelier effect. Acta Metall. Mater. 38, 697–708.

Kuhlmann-Wilsdorf, D., 1999. The theory of dislocation-based crystal plasticity. Philos. Mag. A 79, 955–1008.

Louat, N., 1981. On the theory of the Portevin-Le Chatelier effect. Scripta Metall. 15, 1167–1170.

McCormick, P.G., 1971. The Portevin-Le Chatelier effect in an Al–Mg–Si alloy. Acta Metall. 19, 463–471.

Mesarovic, S.D., 1995. Dynamic strain aging and plastic instabilities. J. Mech. Phys. Solids 43, 671–700.

Nemat-Nasser, S., Guo, W.G., Cheng, J.Y., 1999a. Mechanical properties and deformation mechanisms of a commercially pure titanium. Acta Mater. 47, 3705–3720.

Nemat-Nasser, S., Guo, W.G., Liu, M., 1999b. Experimentally-based micromechanical modeling of dynamic response of molybdenum. Scripta Mater. 40, 859–872.

Nemat-Nasser, S., Isaacs, J.B., 1997. Direct measurement of isothermal flow stress of metals at elevated temperatures and high strain rates with application to Ta and Ta–W alloys. Acta Mater. 45, 907–919.

Nemat-Nasser, S., Li, Y., 1998. Flow stress of F.C.C. polycrystals with application to OHFC Cu. Acta Mater. 46, 565–577.

Neuhäuser, H., Flor, H., 1978. Variation of obstacle strength during stress relaxation of α-brass single crystals. Scripta Metall. 12, 443–448.

Schwarz, R.B., 1979. High-temperature solid-solution strengthening studied through internal friction. In: Haasen, P., Gerold, V., Kostorz, G. (Eds.), Strength of Metals and Alloys, ICSMA 5, Aachen, pp. 953–958.

Seeger, A., 1958. Kristallplastizität. In: Flügge, S. (Ed.), Handbuch der Physik, VII/2. Springer, Berlin, p. 1.

van den Beukel, A., 1980. On the mechanism of serrated yielding and dynamic strain ageing. Acta Metall. 28, 965–969.

van den Beukel, A., 1983. The influence of static and dynamic strain aging on the temperature dependence of the flow stress in solid solutions. Scripta Metall. 17, 659–663.